

## Article

# Seismic Vulnerability Assessment of Historical Masonry Buildings in Croatian Coastal Area

Željana Nikolić <sup>1,\*</sup>, Luka Runjić <sup>2</sup>, Nives Ostojić Škomrlj <sup>1</sup> and Elena Benvenuti <sup>3</sup><sup>1</sup> Faculty of Civil Engineering, Architecture and Geodesy, University of Split, 21000 Split, Croatia; nives.ostojic@gradst.hr<sup>2</sup> Projektni Biro Runjić, 21000 Split, Croatia; lrunjic.ured@gmail.com<sup>3</sup> Engineering Department, University of Ferrara, 44121 Ferrara, Italy; bnvln@unife.it

\* Correspondence: zeljana.nikolic@gradst.hr

**Abstract:** (1) Background: The protection of built heritage in historic cities located in seismically active areas is of great importance for the safety of inhabitants. Systematic care and planning are necessary to detect the seismic vulnerability of buildings, in order to determine priorities in rehabilitation projects and to continuously provide funds for the reconstruction of the buildings. (2) Methods: In this study, the seismic vulnerability of the buildings in the historic center of Kaštel Kamelovac, a Croatian settlement located along the Adriatic coast, has been assessed through an approach based on the calculation of vulnerability indexes. The center consists of stone masonry buildings built between the 15th and 19th centuries. The seismic vulnerability method was derived from the Italian GNDT approach, with some modifications resulting from the specificity of the buildings in the investigated area. A new damage–vulnerability–peak ground acceleration relation was developed using the vulnerability indexes and the yield and collapse accelerations of buildings obtained through non-linear static analysis. (3) Results: A seismic vulnerability map, critical peak ground accelerations for early damage and collapse states, and damage index maps for two return periods have been predicted using the developed damage curves. (4) Conclusions: The combination of the vulnerability index method with non-linear pushover analysis is an effective tool for assessing the damage of a building stock on a territorial scale.

**Keywords:** seismic vulnerability; historical masonry buildings; vulnerability index; pushover analysis; damage index; large-scale assessment

**Citation:** Nikolić, Ž.; Runjić, L.; Ostojić Škomrlj, N.; Benvenuti, E. Seismic Vulnerability Assessment of Historical Masonry Buildings in Croatian Coastal Area. *Appl. Sci.* **2021**, *11*, 5997. <https://doi.org/10.3390/app11135997>

Academic Editor: Marco Vona

Received: 21 May 2021

Accepted: 23 June 2021

Published: 28 June 2021

**Publisher's Note:** MDPI stays neutral with regard to jurisdictional claims in published maps and institutional affiliations.



**Copyright:** © 2021 by the authors. Licensee MDPI, Basel, Switzerland. This article is an open access article distributed under the terms and conditions of the Creative Commons Attribution (CC BY) license (<http://creativecommons.org/licenses/by/4.0/>).

## 1. Introduction

Many countries with moderate to high seismic risks, including Croatia, have old towns with stone or brick masonry buildings, built long before the approval of the first seismic regulations. Some of these towns are categorized as cultural heritage sites and should be preserved for future generations. Strong earthquakes cause significant damage and failure of such buildings. Rehabilitation requires significant financial resources that cannot be allocated suddenly. Therefore, systematic care and planning are necessary to detect the seismic vulnerability of buildings, in order to determine priorities in regard to their rehabilitation and allocate funds for reconstruction.

Evaluating the seismic vulnerability and capacity, as well as the damage state, is a demanding task even for a single building. It requires complex non-linear methods such as nonlinear static (pushover) analyses [1,2], in which the structure is gradually loaded according to a uniform or a modal pattern up to the point of collapse, or incremental dynamic analyses [3], in which ground acceleration is increased up to the point of structural collapse. Both types of analysis allow the determination of the collapse load as well as the monitoring of the damage level, which is continuously increasing because of the nonlinear dissipative processes, including the fracturing and plasticity of the structural components.

Due to the restrictions of the non-linear static analysis for structures that oscillate predominantly in the first mode, multi-modal nonlinear static analysis [4] can be used in the cases of horizontal and vertical irregularities.

An estimation of the seismic vulnerability of a large number of buildings at an urban scale is much more demanding because it is not possible to carry out a nonlinear analysis for all of these buildings.

One of the possible ways to solve this problem is the definition of fragility curves by means of a numerical analysis, coupled with statistical processing of the results. The fragility curves relate the probabilities of exceeding a specific damage measure for a certain intensity [5–7]. Several studies using fragility curves were recently performed to evaluate the seismic vulnerabilities and damage scenarios of urban centers to identify the main criticalities [8–16].

Empirical methods like the damage probability index method [17] and the vulnerability index method [18,19] have also been widely employed to define the vulnerability of urban areas.

Studies based on the damage probability index method [20,21] use probabilistic matrices of damage for the prediction of the damage patterns corresponding to different seismic events. The main finding of the damage probability index method is that certain structural typologies share the same probability of damage for a given intensity of earthquake. Many studies have been developed using different macroseismic scales, such as the Medvedev–Sponheuer–Karnik (MSK) scale, the Mercalli–Cancani–Sieberg (MCS) scale, and the European macroseismic scale (EMS-98) [22]. Among these, the EMS-98 scale is the most commonly used [22], which identifies five categories of damage. These damage categories very roughly estimate damage to both structural and non-structural elements.

Vulnerability assessments based on the vulnerability index method mostly use an improved version of the original Italian GNDT approach, developed by the Italian National Group for the Defense against Earthquakes [19]. It calibrates the weights of vulnerability parameters based on a large database of buildings damaged by past earthquakes [23–25]. To calculate the vulnerability of each building, this approach uses information about geometrical, structural, and material parameters and other relevant characteristics, such as structural typologies, horizontal and vertical irregularities, age, and conservation state.

Another established approach to the estimation of earthquake-induced losses is HAZUS [26,27], originally developed for the building typologies typical of regions in the USA.

A significant contribution to the simulation of earthquake risk scenarios in Europe was achieved by the RISK-UE project [21,28]. This project has developed a methodology for the evaluation of direct and indirect damages caused by different earthquake scenarios and the consequences of the damage. The method has been applied to seven European cities. Moreover, a building classification for typical European buildings has been proposed. According to this method, vulnerability and fragility curves are represented in two ways. The first way is through damage–seismic intensity curves, where the damage is defined in the interval 0–5, whereas the seismic intensity is determined using the EMS-98 macroseismic scale. The second way uses capacity curves, obtained through non-linear analyses of buildings typical of a certain class, for the purpose of deriving the fragility curves. The main difficulty in the application of this approach is how to assign an appropriate class to a particular building.

Most of the aforementioned approaches require the calibration of vulnerability and fragility curves via post-earthquake damage observations. Some other studies have analytically evaluated these vulnerability functions [29].

If the methodology of the vulnerability index is used for the seismic vulnerability assessment, a relation between the vulnerability index, the earthquake intensity, and the damage of the building can be established, using the observation data regarding the damage to buildings induced by past earthquakes [18,30].

Several contributions in the literature discuss various vulnerability assessment methodologies and case studies, in which the level of vulnerability and damage depend on the intensity of the seismic event [31,32]. In particular, we refer to [33] for a comprehensive review of the most relevant vulnerability assessment methods applicable at different scales. The applied approach depends on the study area (settlement, city, region, country) and the available data about the building stock, the purpose of the study, and the seismic hazard and damage levels induced by past earthquakes.

Considering the scarcity of post-earthquake damage observation data, especially in places where there have been no significant recent earthquakes, modern analytical approaches based on non-linear pushover analysis or incremental dynamic analysis offer the possibility to define vulnerability functions and maps independently of the available information about the damage level.

In general, methodologies for assessing seismic vulnerability and earthquake risk are being devised and applied in developed countries with high seismic risk that are able to allocate significant financial resources for seismic risk management. Croatia is a country with relatively limited resources dedicated to seismic risk prevention and management. To date, there is no technical regulation that prescribes the rules for assessing seismic vulnerability or seismic risk. The main contributions to the investigation of the seismic vulnerability mainly are drawn from individual research work, mainly focusing on the classification of the building stock and the development of vulnerability curves in the cities of Zagreb and Osijek. The vulnerability assessment in Zagreb concerns building classification and the development of fragility curves, whereas damage probability matrices related to earthquake intensity and structural systems have been used in assessments of damage according to the EMS-98 scale [34]. The vulnerability assessment of old confined masonry buildings in Osijek was recently performed using vulnerability indexes with behavior modifiers and damage states assessed according to EMS-98 [35]. An approach based on damage index coefficients and single-degree-of-freedom systems was applied to a historical building located in Tvrdja, Osijek [36]. Mean damage levels,  $\mu D$ , according to the macro-seismic method [35] and the analytical capacity spectrum method, have been used to estimate the vulnerability of a few blocks of buildings, representative of the Osijek city, and the relevant fragility curves have been calculated [37]. All these investigations consider masonry buildings that are typical of continental Croatia. In addition, they have mostly estimated the damage for some building typologies merely based on the structural system and period of construction, while neglecting other relevant peculiarities.

Cities and settlements on the Adriatic coast have been gradually built and expanded over the centuries, and some of them, such as Split, are almost two millennia old. Some of these settlements are old towns with massive stone masonry buildings, which are often protected and declared architectural heritage sites. Around the cores of these sites, settlements have spread, especially since the second half of the 20th century. Buildings in old city cores are very sensitive to earthquakes for several reasons. Firstly, they were constructed with unconfined stone walls and wooden ceilings, which cannot effectively transmit earthquake force. Secondly, their state of maintenance is often critical, considering their age. On the other hand, these city centers are densely populated, and the large number of tourists during the summer conspicuously increases the number of inhabitants. The seismic vulnerability assessment of the buildings of such towns and cities is crucial for the safety of permanent inhabitants and tourists.

In the present study, a seismic vulnerability assessment approach based on the calculation of seismic vulnerability indexes was applied to Kaštel Kambelovac, a Croatian settlement located in the coastal Dalmatian area. The town consists of a historical core with stone masonry buildings built between the 15th and 19th centuries and more peripheral buildings built from the beginning of the 20th century up to the present. These buildings were erected according to different technical regulations as they date from different periods, namely, before 1948, from 1949 to 1964, from 1964 to 1982, from 1982 to

2005, and, finally, from 2005 onwards. This paper presents the development of a methodology for a seismic vulnerability assessment and its application to the stone masonry buildings in the historical core. The investigation was supported by the Interreg Italy-Croatia project “Preventing, managing, and overcoming natural-hazards risks to mitigate economic and social impact” (PMO-GATE) in which multi-hazard risks caused by earthquakes, floods caused by rising sea levels due to climate change, and extreme sea waves are analyzed.

The seismic vulnerability method applied in this work was derived from the Italian GNDT approach, with some modifications resulting from specific aspects of the buildings and the construction materials typical of the investigated area. Instead of the field observation of the damage state caused by past earthquakes, a static non-linear pushover analysis was performed for the typical buildings at the test site. Furthermore, the yield and collapse accelerations were determined and, subsequently, new relations between damage, vulnerability, and peak ground acceleration were derived. The damage index was expressed in the 0–1 space by means of a tri-linear law defined by the yield acceleration,  $PGA_y$ , which represents the beginning of the damage, and the acceleration of the collapse of the building,  $PGA_c$ .

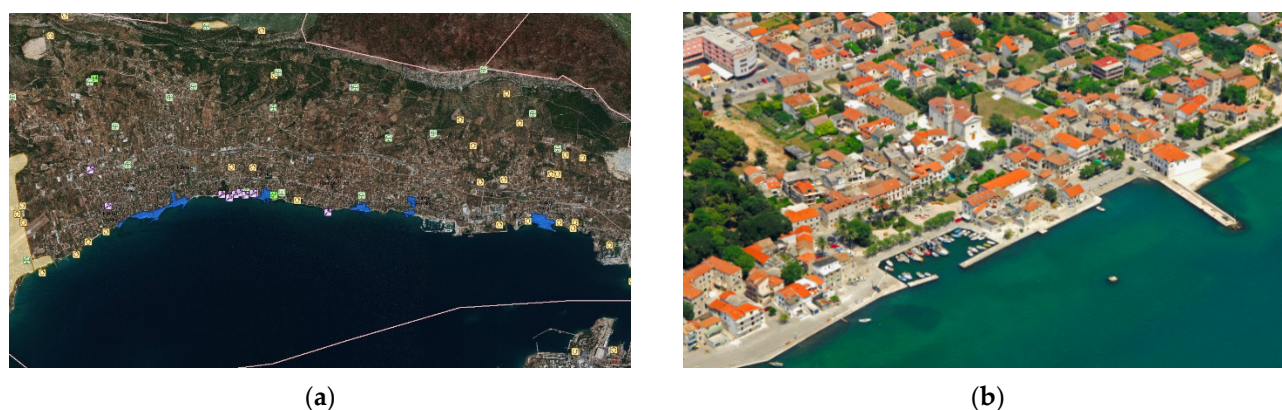
Seismic vulnerability indexes for the historical masonry buildings in a typical settlement located along the Dalmatian coast were computed. These indexes were used to build a seismic vulnerability map of the area. New damage curves for the estimation of the damage to the building under specific seismic conditions were derived and the results were presented for two return periods, according to EC8.

The proposed approach has some similarities with a hybrid procedure for the definition of seismic vulnerability in Mediterranean cross-border urban areas [38]. However, in that paper [38], the vulnerability curve proposed by Guagenti and Petrini [23] was calibrated using the numerical results for prototype buildings that were representative of the most widespread building typologies [38]. On the contrary, the investigation presented in this study was based on the estimation of the damage state through non-linear pushover analysis of a large number of buildings, more specifically, a total of 11 buildings in the test area. Furthermore, a new damage–vulnerability–peak ground acceleration law has been derived.

## 2. Seismic Vulnerability Assessment of the Test Site

### 2.1. Description of the Test Site

The selected test site for the application of the methodology developed in the project is Kaštel Kambelovac, one of the seven settlements comprising the town of Kaštela (Figure 1). The relevant area covers around 45,000 square meters and includes more than 400 buildings. The settlement consists of a historical core with stone masonry buildings built between the 15th and 19th centuries (Figure 2) and of the parts outside the historical core dating from the beginning of the 20th century to the present (the north, east and, west parts are shown in Figure 3). These buildings were constructed in different periods according to different technical regulations. The oldest buildings were constructed before 1948; then, some blocks were erected from 1949 to 1964, from 1964 to 1982, and from 1982 to 2005. The most modern buildings have been built from 2005 onwards.



(a)

(b)

**Figure 1.** Town of Kaštela: (a) protected architectural heritage of the town of Kaštela; (b) a view of an old historical core, Kastel Kambelovac [39].

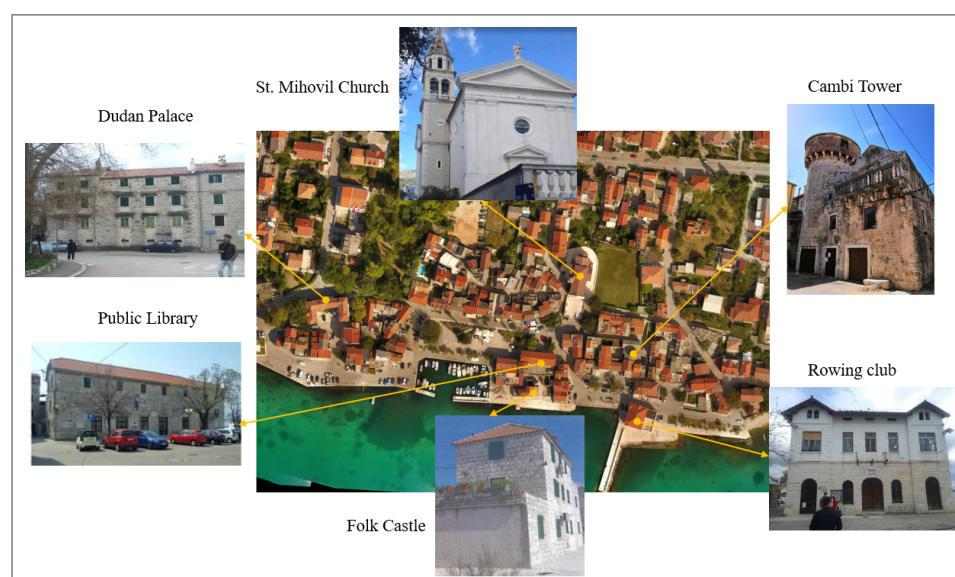


**Figure 2.** Historic center with typical buildings, Kaštela Kambelovac.

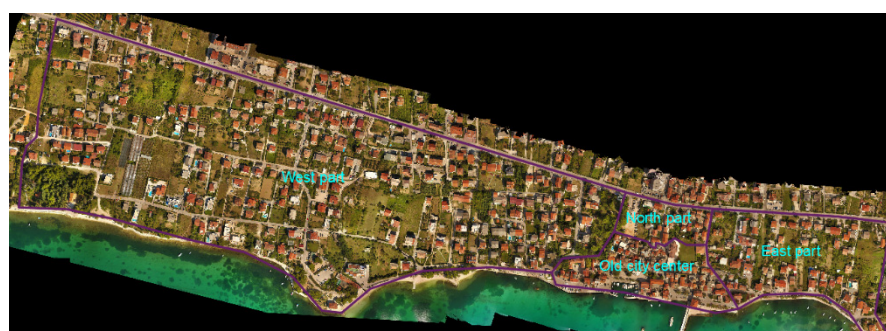


**Figure 3.** Kaštela Kambelovac test site with four characteristic parts.

The buildings in the historic center were constructed with stone blocks with mortar joints, the walls' thickness being between 45 and 75 cm. The structural frame is characterized by wooden floors consisting of beams and a wooden floor covering. The quality of the walls depends on the processing of the stone, their way of stacking, and on the quality of the mortar in the joints. The walls' textures vary from rough non-squared stone masonry of variable size arranged in a chaotic manner, to well-organized masonry made of well-shaped or cut blocks of almost uniform size (Figure 4). The mortar is mainly of a low



quality. The buildings were constructed without confining elements and with poor connections between the walls and floors. Some of these buildings were then reconstructed and wooden floors were replaced with monolith reinforced concrete plates.

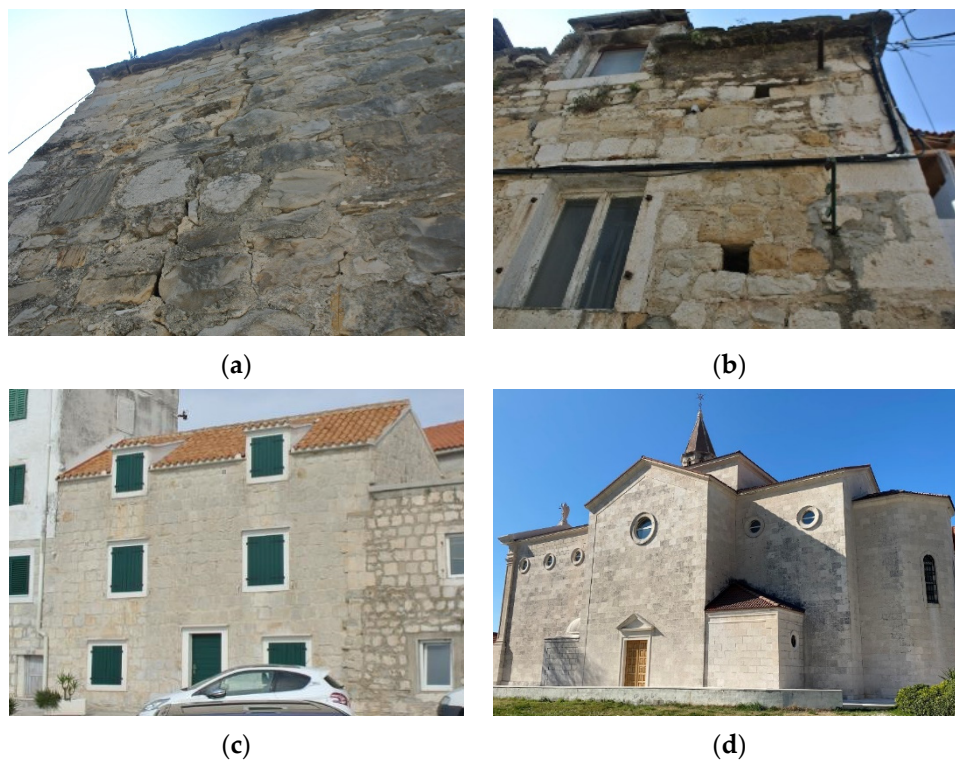


**Figure 4.** Examples of wall textures of stone masonry buildings: (a) non-squared roughly shaped stone masonry of various sizes arranged in chaotic manner; (b) wall composed of disorganized roughly shaped stones; (c) walls made of natural well-worked homogenous squared stones accurately executed; (d) walls of St. Mihovil church, composed of well-organized cut blocks.

Some buildings are in very poor condition, without mortar in the joints between the stone blocks, significant cracks in the load-bearing walls and, in some cases, with collapsed roofs (Figure 5). Several buildings are completely demolished.





**Figure 5.** Current state of buildings in the historic centre: (a) damage to Cambi tower; (b) completely demolished building; (c,d) significant cracks in the load-bearing walls of residential buildings.

The general problem with assessing the earthquake vulnerability of these buildings is that most of them are private residential buildings. Some of them have been reconstructed and upgraded. The most common reconstruction interventions are the replacement of flexible ceilings with RC slabs and the replacement of old roofs. In some buildings, new floors were added during the reconstruction. In some buildings, new floors were added during the reconstruction. These processes were often carried out illegally and were not documented. The lack of documentation is also a major issue in defining the structural characteristics of these buildings.

Generally, buildings have a low level of safety with regard to earthquake events. The lack of free space in the enclosed area resulted in a high urban density. The buildings lean one against the other and have merged into blocks with narrow streets. This high density represents an additional safety problem for the population in the event of an earthquake.

## 2.2. Collection of the Geometrical, Material, and Structural Data

The seismic assessment of buildings in the test area requires the knowledge of their geometrical, material, and structural characteristics. The methodology for data collection was organized as follows:

- Investigation of the buildings using historical documentation [40] and archival documentation of the town of Kaštela;
- Detailed survey of geometrical characteristics, architectural measurements, and creation of architectural drawings (floor plans and cross sections);
- Identification of structural systems and materials through visual inspection, using archive documentation, literature, and thermographic imaging in the several specific cases where, due to non-documented reconstructions, it was not possible to recognize the material and structural characteristics of the buildings;
- Characterization of the soil type by means of a geophysical survey.

Additional assistance came from high-resolution geodetic maps of the test site with precise plan dimensions, from Google Maps with Street View options, and also a map of the area made in 1968 that allowed the identification of reconstructions.

Investigations of archival documentation and visual inspection were used to detect the main structural features crucial to the seismic vulnerability assessment, such as the type and configuration of the structural system, the texture and quality of masonry walls based on the distribution of blocks and mortar joints, as well as their thickness, the mortar quality, the type of floors, and the floor–wall connections. Furthermore, other important aspects that were investigated were the resistance along two main horizontal directions

based on estimates of the maximum resistant shear of the structure, the position and foundations of the building, its horizontal and vertical configurations, the maximum distance among the walls, the typology and weight of the roof, the presence of non-structural elements, and the state of conservation. The mechanical properties of the materials (stone walls, mortar) were taken from the literature [41,42]. A valid seismic regulation in the past was also used to identify the material properties in the case of reconstructions.

### 2.3. Seismic Vulnerability Assessment Using the Vulnerability Index Method

The adopted vulnerability index method was based on the original vulnerability index method for masonry structures developed by the Italian National Research Council and the Italian National Group for the Defense Against Earthquakes (GNdT) from 1984 onwards [18,19].

The method consists in filling in a survey with data relating to 11 geometrical and structural vulnerability parameters, the calculations of those parameters, and finally, the calculation of the vulnerability index for the building. The main parameters consider the type and organization of the resistant system, the quality of resistant system, the conventional resistance along two main horizontal directions of the building based on the estimation of the maximum resistant shear of the structure, the position of the building and foundations, the typology of floors, the planimetric and elevation configuration, the maximum distance among the walls, the typology and weight of the roof, the presence of non-structural elements, and the state of conservation. For each parameter, the surveyor must judge the condition among four possibilities, from “A”, corresponding to an optimal condition, to “D”, meaning a bad condition. For each judgment, the method provides a numerical score. Weight coefficients are then used, relating to each parameter to account for the relative importance of each parameter in the global definition of vulnerability. Finally, a vulnerability index  $I_V$  is calculated in the form:

$$I_V = \sum_i s_{vi} w_i, \quad (1)$$

where  $s_{vi}$  is the numerical score for each class and  $w_i$  is the weight of each parameter. This vulnerability index is then normalized in a 0–100% range. A low index means that the structure is not particularly vulnerable and has a high capacity under seismic action, whereas a high index shows that the structure is vulnerable and has low seismic capacity.

The method was improved with the modifications proposed for the region of Tuscany in 2003 [43] to consider the possible substitution of the original light timber floors with heavier reinforced-concrete slabs. Field observations of the damage states of heritage buildings after earthquakes in the past 30 years has indeed shown that the replacement of timber floors with heavier concrete slabs, when performed on low quality masonry buildings, can substantially change the dynamic behavior of the structures, because it adds a considerable mass on the top of the building, thus increasing the overall in-plane stiffness. These changes can cause the collapse of the structure under earthquake excitation. Therefore, researchers on the Tuscan region corrected the vulnerability index method and updated the weights of parameters 1, 5, and 9. In particular: (1) in parameter 1, the weight changes from 1 to 1.5; (2) in parameter 5, the weight changes from a range 0.5–1 to the range 0.5–1.25, in particular, if heavier floors, such as concrete slabs, are supported by not-so-resistant masonry walls, the weight coefficient is 1.25; (3) in parameter 9, the weight changes from the range 0.5–1 to 0.5–1.5, and the calculation of the weight is the same as the original interval (0.5–1.0), where the weight is 1.25 if a heavier roof, such as a concrete slab, is supported by weak masonry walls, and it is 1.5 if there is also a heavy floor just below the roof.

The present work uses the aforementioned modified weights proposed for the Tuscan region [43]. The weights of all the other parameters are assumed as in the original vulnerability index method.



The vulnerability parameters, their numerical score values, and weight coefficients are shown in Table 1. The maximum value of the vulnerability index  $I_v$  is 438.75.

**Table 1.** Vulnerability parameters and their weights.

Parameter	Score ( $s_{vi}$ )				Weight ( $w_i$ )
	A	B	C	D	
Type and organization of the resistant system (P1)	0	5	20	45	1.50
Quality of the resistant system (P2)	0	5	25	45	0.25
Conventional resistance (P3)	0	5	25	45	1.50
Position of the building and foundation (P4)	0	5	25	45	0.75
Typology of floors (P5)	0	5	15	45	var.
Planimetric configuration (P6)	0	5	25	45	0.50
Elevation configuration (P7)	0	5	25	45	var.
Maximum distance among the walls (P8)	0	5	25	45	0.25
Roof (P9)	0	15	25	45	var.
Non-structural elements (P10)	0	0	25	45	0.25
State of conservation (P11)	0	5	25	45	1.00

Based on the presented methodology, a vulnerability index Excel sheet was created and used to compute the vulnerability indexes of masonry historical buildings in the test site.

#### 2.4. Seismicity of the Area

The seismic hazard level for Croatia can be evaluated through two maps, expressed in terms of the peak horizontal ground acceleration during an earthquake, one map for a return period of 475 years, used in designing earthquake-resistant buildings, and the other one for a return period of 95 years, used to check the fundamental requirements of damage state limitations [44]. The maps were integrated into the National Annex in HRN EN 1998-1:2011 [45]. In the Kaštela area, the seismic hazard, measured via the peak ground acceleration for the soil type A, is equal to  $a_g = 0.22$  g and  $a_g = 0.11$  g for the return periods of 475 and 95 years, respectively. In Croatia, the type 1 response spectrum for an earthquake magnitude higher than 5.5 was adopted.

According to EN 1998-1:2011 [41] and HRN EN 1998-1:2011 [45], the soil factor  $S$ , for ground types different from A, increases the ordinate of the elastic response spectrum. The real hazard for a certain location can be obtained by combining the peak ground acceleration for ground type A with the soil factor  $S$ , describing the influence of local ground conditions on the seismic action.

The test site was investigated to classify soils according to [46]. Three seismic lines were acquired in May 2019 in the test site [47] (Figure 6). A velocity analysis based on travel time tomography of P, SV, and SH arrivals, acquired on three seismic lines on the shore of the Kaštela Bay, was performed. The  $V_{s,30}$  map along each line was also computed by averaging the vertical  $V_{sH}$  tomographic values from the surface to a depth of 30 m. Relatively high obtained values, between 1.2 and 1.7 km/s, indicate the presence of shallow hard rock [14], which can be classified as soil type A according EN 1998-1:2011 [46]. Considering the results obtained along the three investigated lines and given the size of the test area, the seismic hazard was assumed to be constant for all buildings in the area.



**Figure 6.** (a) Location of the Kaštela City on the Dalmatian coast. (b) Position of the seismic lines in the historic center of Kaštela [47].

## 2.5. Vulnerability Index Results

### Historical Core

The vulnerability indexes for 75 buildings in the historical core were calculated and all collected data were digitalized. Some of these buildings are located in several cadastral parcels and have different owners, but they were put in the same class because of their structural integrity. To improve the interpretation of the results, these individual vulnerability parameters, as well as other important input information, were integrated into a geographical information system (GIS) tool. The GIS software adopted in this study was the open-source suite ESRI ArcGIS Runtime 100.4 v1, in which geo-referenced graphical data (vectorized information and orthophoto maps) were combined with building parameter information.

The buildings were divided into 4 vulnerability classes: low vulnerability for  $I_v < 30$ , medium-low vulnerability for  $30 < I_v < 45$ , medium-high vulnerability for  $45 < I_v < 60$ , and high vulnerability for  $I_v > 60$ . Figure 7 shows the vulnerability map of the area, whereas the distribution of the vulnerability is shown in Figure 8. Most buildings in the historical core belonged to the high vulnerability class (25%) and to the medium-high vulnerability class (47%). A small number of buildings were classified as medium-low vulnerability (21%). Only a few buildings were of low vulnerability (7%), and these were old stone buildings that were reconstructed. Buildings with vulnerability index of 45 and larger were considered highly vulnerable, as expected, given the age of the town center. The indexes ranged from 11.1, corresponding to one of the newer houses that was completely renovated at the boundary of the core, to 76.9, the vulnerability index of the Cambi tower. Houses made of poorly connected walls, with flexible floor structures, irregular in layout and height, were revealed to be more endangered. In addition to these basic aspects, the degree of general preservation of the building and the presence of subsequent reconstructions significantly affected the vulnerability indexes.

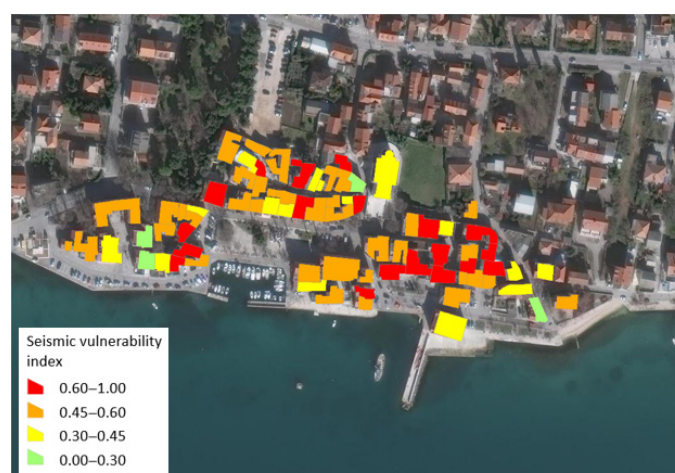


**Figure 7.** Vulnerability map of the historical core.

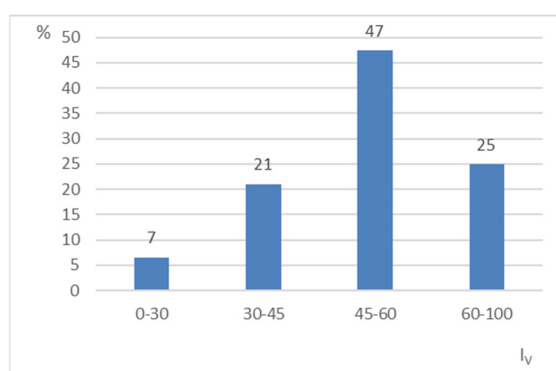


**Figure 8.** Vulnerability index distribution in the historical core.

The investigation of the parameters necessary for evaluating the seismic vulnerability index allows us to characterize and draw some indicators that can help to better understand the overall vulnerability results. The spatial distribution of these parameters was analyzed and the results are shown in Figure 9.

We first focused on parameter “type and organization of the resistant system”, which measures the presence of connections among perpendicular walls and connections among floors or roofs in masonry buildings, which are necessary to ensure the three-dimensional box behavior of the building. We detected that about 77% of the buildings were made without any confining elements and with poorly connected stone walls (class D), whereas 21% were also made without confining elements but had strongly connected walls (class C). Only 1% were in class A, having been reconstructed. Most buildings were made without confining elements (classes C and D), this being one of the main aspects that can lead to significant damage and to the separation of the walls.

The “quality of the resistant system” parameter is based on the type of masonry, considering the type of material, the shape of the elements, and the homogeneity of the walls. Figure 9b shows the distribution of the buildings between vulnerability classes A to D, with 3%, 3%, 57%, and 37% of buildings, respectively. The majority of them belonged to classes C and D, indicating medium to high vulnerability.

The “conventional resistance” parameter estimates the maximum shear strength of the structure, accounting for the resistant area of the walls in the two main horizontal directions. As shown in Figure 9c, the buildings were distributed between vulnerability classes A to D, with 1%, 16%, 68%, and 15% of the buildings, respectively.

The “position of the building and foundation” parameter considers the influence of the local morphology of the site and the natural slope of the ground. Its distribution in Figure 9d showed a low level of vulnerability. Specifically, 57% of buildings were in class

A and 43% were in class B. The reason for such a distribution is the presence of solid soil of type A and the relatively small slope of the terrain.

The “typology of floors” parameter evaluates the in-plane stiffness of the floor and the presence of efficient floor-to-wall connections. The buildings were distributed between vulnerability classes A to D, with 19%, 0%, 3% and 78% of buildings, respectively (Figure 9e). The reason for this high percentage of buildings in class D is the presence of wooden floors which were poorly connected to the walls.

Regarding the parameter of “planimetric configuration”, which measures the regularity of the planimetric shape of the building, 8%, 17%, 23%, and 52% of the buildings were distributed in vulnerability classes A to D, respectively (Figure 9f). The most populated classes were C and D, because a high level of horizontal irregularity was detected.

The “elevation configuration” parameter evaluates vertical regularity through the analysis of the stiffness of different floors, the presence of porticos, lodges, towers, and other structural elements which affect the distribution of the masses at each floor. In terms of this parameter, 19%, 11%, 41%, and 29% of the buildings belonged to vulnerability classes A to D, respectively, as displayed in Figure 9g, with classes C and D proving to be most relevant.

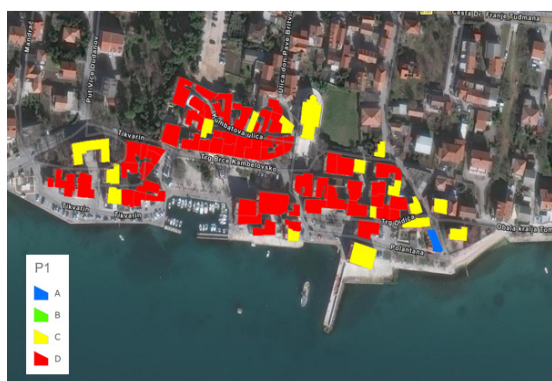
The “maximum distance among the walls” parameter validates the presence of structural walls orthogonally connected to transversal ones. The buildings in the historical core had a favorable distribution, as most of them belonged to classes A and B, with 69% in class A, 12% in class B, 13% in class C, and 5% in class D, as shown in Figure 9h.

In terms of the parameter “roof”, which evaluates the roof’s typology and weight, buildings were distributed among vulnerability classes A to D, with 9%, 40%, 15%, and 36% of the buildings, respectively (Figure 9i).

The presence of “nonstructural elements”, which can cause damages due to falling, highlighted an area of high vulnerability because most buildings had weakly connected nonstructural elements and belonged to classes C and D. The distribution shown in Figure 9j was 12%, 0%, 53%, and 35% for classes A to D, respectively.

The “state of conservation” parameter analyzes the condition of the building and the presence of cracks in structural walls. The relevant distribution, shown in Figure 9k, was as follows: 27% were in class A, 0% in B, 45% in C, and 28% were in class D. Most old stone masonry buildings, which have not yet been reconstructed, are in a bad condition and belong to classes C and D, whereas reconstructed buildings are in class A.

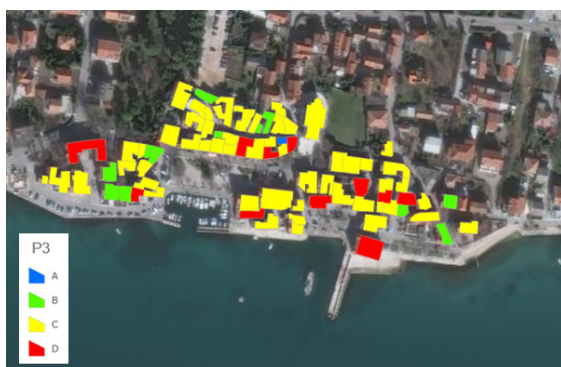




(a)



(b)



(c)



(d)



(e)



(f)



(g)



(h)

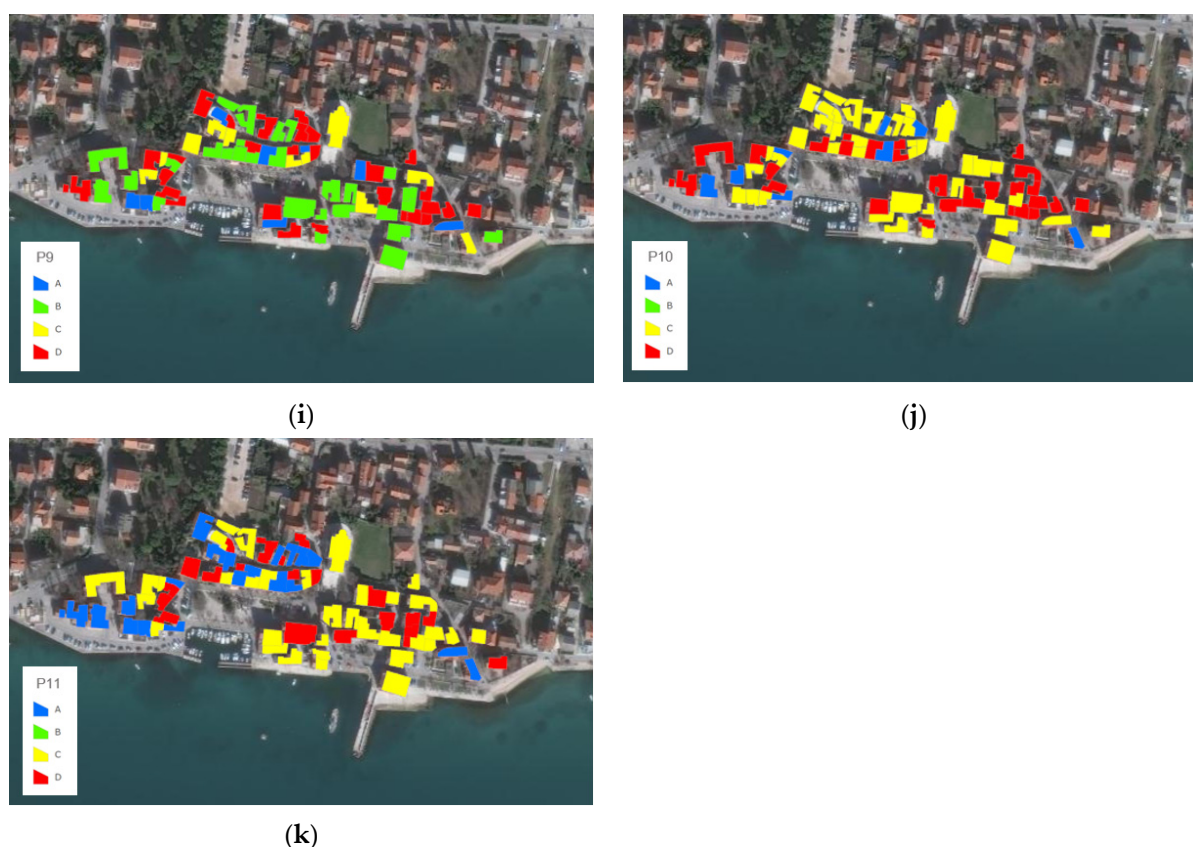


**Figure 9.** Spatial distribution of the 11 parameters that comprise the seismic vulnerability index: (a) type and organization of the resistant system; (b) quality of the resistant system; (c) conventional resistance; (d) position of the building and foundation; (e) typology of floors; (f) planimetric configuration; (g) elevation configuration; (h) maximum distance among walls; (i) roof; (j) non-structural elements; (k) state of conservation.

### 3. Development and Calibration of Vulnerability Model

#### 3.1. Vulnerability Model

The vulnerability index is not a relevant indicator of seismic risk because it does not give information about the behavior of the building under a specific seismic action. The seismic risk of buildings is often expressed by the damage caused by an earthquake of a certain intensity. Alternatively, it can be formulated in terms of a seismic safety index, defined as the ratio between the peak ground acceleration corresponding to the collapse of the structure and the design ground acceleration. In this paper, an approach based on the evaluation of the damage to the building was applied.

Several studies established correlations between the vulnerability index, peak ground acceleration, or macro-seismic intensity, and the damage index. They present a cause–effect relation, where the earthquake is the cause and the damage is the effect. Therefore, vulnerability relates the ground acceleration to a certain level of damage. Two limit-levels of acceleration are important for the damage analysis: the acceleration corresponding to the beginning of the damage to a structure, and the acceleration corresponding to the collapse. The level of damage varies in the  $[0, 1]$  space.

This study uses the approach developed by Guagenti and Petrini [23], who derived a relation between damage, acceleration, and the vulnerability index by observing the damage to masonry buildings under real earthquakes. They studied a set of damaged masonry buildings in the historical city center of the towns of Venzona (Udine, Intensity IX MCS, May 1976 earthquake), Tarcento, and San Daniele (Udine, Intensity VIII MCS, May 1976 earthquake); they also considered some other buildings from the 1984 Parco d’Abruzzo earthquake (Intensity VII MCS). The level of damage to each building, as well

as the level of the ground acceleration, were accounted for. Corresponding acceleration/damage laws can be represented with smooth vulnerability curves, such as the one shown in Figure 10.

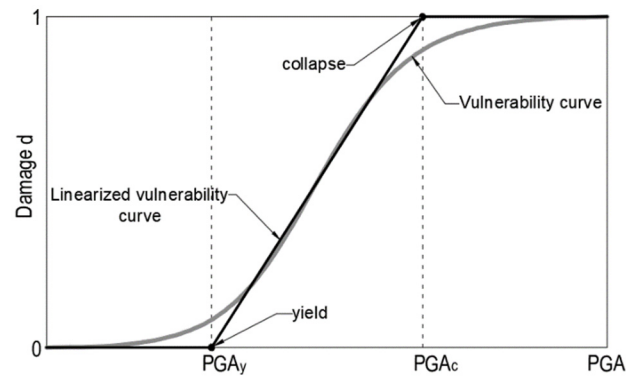


**Figure 10.** Vulnerability curve and its idealization.

For simplicity, Guagenti and Petrini substituted the vulnerability curve with a tri-linear law defined by the values of the peak ground acceleration corresponding to early damage,  $PGA_i$ , and to the collapse,  $PGA_c$ , as follows:

$$d = \begin{cases} 0 & PGA < PGA_i \\ (PGA - PGA_i) / (PGA_c - PGA_i) & PGA_i \leq PGA \leq PGA_c \\ 1 & PGA > PGA_c \end{cases} \quad (2)$$

By means of this equation, the definition of the beginning of the damage and the collapse of buildings are related to the two values of acceleration.

In this work, instead of a field observation of the damage caused by past earthquakes, a static non-linear pushover analysis was performed for the buildings at the test site; thus, the yield and collapse acceleration were determined. Then, using the previously computed vulnerability indexes and yield and collapse accelerations, new damage–vulnerability–peak ground acceleration relationships were derived. The damage index is expressed in the [0–1] space via a tri-linear law, shown in Figure 11, defined by two points: yield acceleration  $PGA_y$ , which represents the beginning of the damage ( $d = 0$ ), and acceleration for the collapse of the building  $PGA_c$  ( $d = 1$ ).

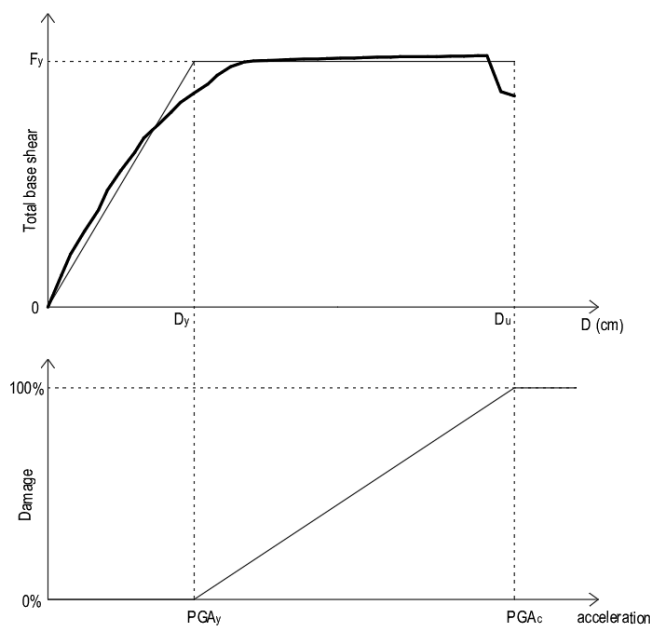


**Figure 11.** Pushover curve and tri-linear acceleration/damage law.

### 3.2. Static-Nonlinear Pushover Analysis of Representative Buildings

Peak ground accelerations at the yield and the collapse of the structure were evaluated through static non-linear pushover analysis, according to Eurocode 8 [41] and the corresponding Croatian standards [45,48]. Eleven buildings in the town center, representative of the structural and material characteristics of the test area, were analyzed.

The analysis was carried out with TREMURI software [49,50], in which the building is modelled as a spatial structure where the walls resist to both vertical and horizontal loads. Walls are modeled by means of non-linear two-node macro-elements, representing whole masonry panels and piers. The macro-element considers both the shear-sliding damage failure mode and its evolution. It accounts for strength and stiffness degradation, and rocking mechanisms, whereas the toe crushing effect is modeled by means of a phenomenological non-linear constitutive law with stiffness degradation under compression.

The horizontal structures, such as floors, vaults and ceilings, transfer their vertical loads to the walls and transmit the horizontal actions to the walls. In this way, the structure is modeled by assembling the walls and the horizontal structures, both lacking bending rigidity outside of the level. Horizontal structures can have membrane stiffness or can be regarded as rigid. For each slab's typology, the connection of the structural components should be defined. A good connection to the masonry contributes to the resistance of the global system. In addition, the floor can divide its mass in a single direction or along two directions of the floor. If the floors possess bi-directional stiffness, it is necessary to indicate the vertical load percentage for the principal direction. The floors are modeled as orthotropic membrane three-node elements, with two degrees of freedom per node (displacements  $u_x$  and  $u_y$ ), which are associated with a warping direction. This enables us to model both flexible and rigid floors.

The same rules for floors also apply to roofs. A roof can be modeled as a part of a bearing system or just as a load-distributing frame.

The response of the structure is investigated along the two geometrical orthogonal axes, in both the positive and negative directions. Non-regular distribution of the masses inside the structure is considered by means of the assumption of an eccentricity of the lateral loads, equal to  $\pm 5\%$  of the maximum floor dimension at each level. Three lateral load distributions—uniform, linear and modal distribution—and considering positive and negative eccentricities led to a total of 36 analyses.



Each pushover analysis resulted in an MDOF capacity curve, which represents the relation between base shear force and the displacement of a control node placed at the top of the building. The pushover curve was scaled according to the N2 method described in Annex B of Eurocode 8 [46] using the transformation factor  $\Gamma = \sum m_i \Phi_i / \sum m_i \Phi_i^2$ , where  $\Phi_i$  is the  $i$ -th component of the eigenvector and  $m_i$  is the mass of the node  $i$ . For the actual base shear force  $F$  and the corresponding top displacement of the structure  $d$  of the MDOF system, the values  $F^* = F/\Gamma$  and  $d^* = d/\Gamma$  represent the base shear force and the displacement of the equivalent SDOF system, respectively.

After the transformation of the MDOF curve in the SDOF one, a bilinear force–displacement diagram was obtained. The yield force  $F_y^*$ , representing the actual strength of an idealized system, is equal to the base-shear force at the formation of the plastic mechanism. The initial stiffness was determined assuming an area equivalence between the equivalent and the bilinear system. The yield displacement of the bilinear SDOF system  $d_y^* = 2(d_m^* - E_m^*/F_y^*)$  was obtained from the deformation energy  $E_m^*$  up to the formation of the plastic mechanism. The mass  $m^*$ , the stiffness  $k^*$ , and the period  $T^*$  of the equivalent SDOF system can be obtained as follows:

$$m^* = \sum_{i=1}^n \Phi_i^* m_i; \quad k^* = \frac{F_y^*}{d_y^*}; \quad T^* = 2\pi \sqrt{\frac{m^*}{k^*}}, \quad (3)$$

The spectral yielding acceleration  $S_{ay}$  and the elastic spectral acceleration  $S_{ae}$  of an elastic SDOF with period  $T^*$  are calculated as:

$$S_{ay} = \frac{F_y^*}{m^*}; \quad S_{ae} = S_{ae}(T^*) \quad (4)$$

Reduction factor  $R_\mu$  is expressed as:

$$R_\mu = \frac{S_{ae}}{S_{ay}} \quad (5)$$

and used to calculate the displacement ductility factor:

$$\begin{aligned} \mu_r &= (R_\mu - 1) \frac{T_c}{T^*} + 1; & T^* < T_c \\ \mu_r &= R_\mu; & T^* \geq T_c \end{aligned} \quad (6)$$

Spectral inelastic demand acceleration  $S_{ai}$  and displacement  $S_{di}$  were derived as follows:

$$S_{ai} = \frac{S_{ae}}{R_\mu(\mu_r, T)}; \quad S_{di} = \frac{\mu_r}{R_\mu(\mu_r, T)} S_{de} = \mu_r \frac{T^2}{4\pi^2} S_{ai}. \quad (7)$$

The values of peak ground acceleration  $PGA_y$  and collapse acceleration  $PGA_c$  are calculated from the corresponding displacements according to the following procedure.

The displacement demand  $d^*$  was cast as a function of the spectral elastic displacement  $S_{de}(T^*)$  using the following analytical relationship:

$$\begin{aligned} d_r^* &= \left[ 1 + (R_\mu - 1) \frac{T_c}{T^*} \right] \frac{S_{de}(T^*)}{R_\mu}; & T^* < T_c \\ d_r^* &= S_{de}(T^*); & T^* \geq T_c \end{aligned} \quad (8)$$

The reduction factor can be calculated again as a function of the actual ductility  $\mu$  of SDOF system in the form:

$$\begin{aligned}\bar{R}_\mu &= 1 + (\mu - 1) \frac{T^*}{T_c} ; \quad T^* < T_c \\ \bar{R}_\mu &= \mu ; \quad T^* \geq T_c\end{aligned}\quad (9)$$

Given the yielding displacement  $d_y^*$  is associated with the early damage state and ultimate displacement  $d_u^*$  with the collapse; the early damage ductility  $\mu_y$  and collapse ductility  $\mu_c$  are expressed as:

$$\mu_y = 1 ; \quad \mu_c = \mu_u = \frac{d_u^*}{d_y^*} \quad (10)$$

The associated spectral displacements can be calculated from Equation (8):

$$S_{de,y}(T^*) = \frac{d_y^* \bar{R}_\mu(\mu_y)}{[\bar{R}_\mu(\mu_y) - 1] \frac{T_c}{T^*} + 1} ; \quad S_{de,c}(T^*) = \frac{d_u^* \bar{R}_\mu(\mu_c)}{[\bar{R}_\mu(\mu_c) - 1] \frac{T_c}{T^*} + 1} \quad (11)$$

The spectral accelerations is given as:

$$S_{ae,y}(T^*) = \frac{4\pi}{T^{*2}} S_{de,y}(T^*) ; \quad S_{ae,c}(T^*) = \frac{4\pi}{T^{*2}} S_{de,c}(T^*) \quad (12)$$

According to Eurocode 8, depending on the period, the elastic spectral acceleration is defined by the following expressions:

$$\begin{aligned}S_{ae}(T) &= a_g S [1 + T/T_B (\eta \cdot 2.5 - 1)], \quad 0 \leq T \leq T_B \\ S_{ae}(T) &= a_g S \eta \cdot 2.5, \quad T_B \leq T \leq T_C \\ S_{ae}(T) &= a_g S \eta \cdot 2.5 T_C / T, \quad T_C \leq T \leq T_D \\ S_{ae}(T) &= a_g S \eta \cdot 2.5 (T_C T_D / T^2), \quad T_D \leq T \leq 4s\end{aligned}\quad (13)$$

Generally, Equations (13) can be written in the form:

$$S_{ae}(T) = PGA f_i(T) \quad (14)$$

Here,  $PGA = a_g$  is peak ground acceleration, whereas  $f_i$  ( $i = 1, \dots, 4$ ) represents the function which defines four different branches of the elastic response spectrum and depends on the period  $T$ , soil factor  $S$ , and damping correction factor  $\eta$ , and the characteristics periods  $T_B$ ,  $T_C$ , and  $T_D$  represent the lower and upper limits of each spectral acceleration branch. The peak ground accelerations  $PGA_y$  and  $PGA_c$ , corresponding to the yield displacement and to the ultimate displacement, respectively, can now be calculated in the form:

$$PGA_y = \frac{S_{ae,y}(T^*)}{f_i(T)} ; \quad PGA_c = \frac{S_{ae,c}(T^*)}{f_i(T)} \quad (15)$$

The procedure of the evaluation of the yield and the collapse acceleration is shown for the building of the Public Library, a stone masonry structure built in the 19th century, in Figure 12. It has three floors (ground floor, first floor, and attic) and is intended for public usage. It consists of a library and a hall for events on the ground floor and offices on the first floor. The structure is made of stone walls and wooden floors. The walls were built of natural carved stone, 50-cm thick, with medium-quality mortar. The roof above the attic was made as a wooden structure with double-sided water lines and a tile cover. The building is irregular in plan and elevation.

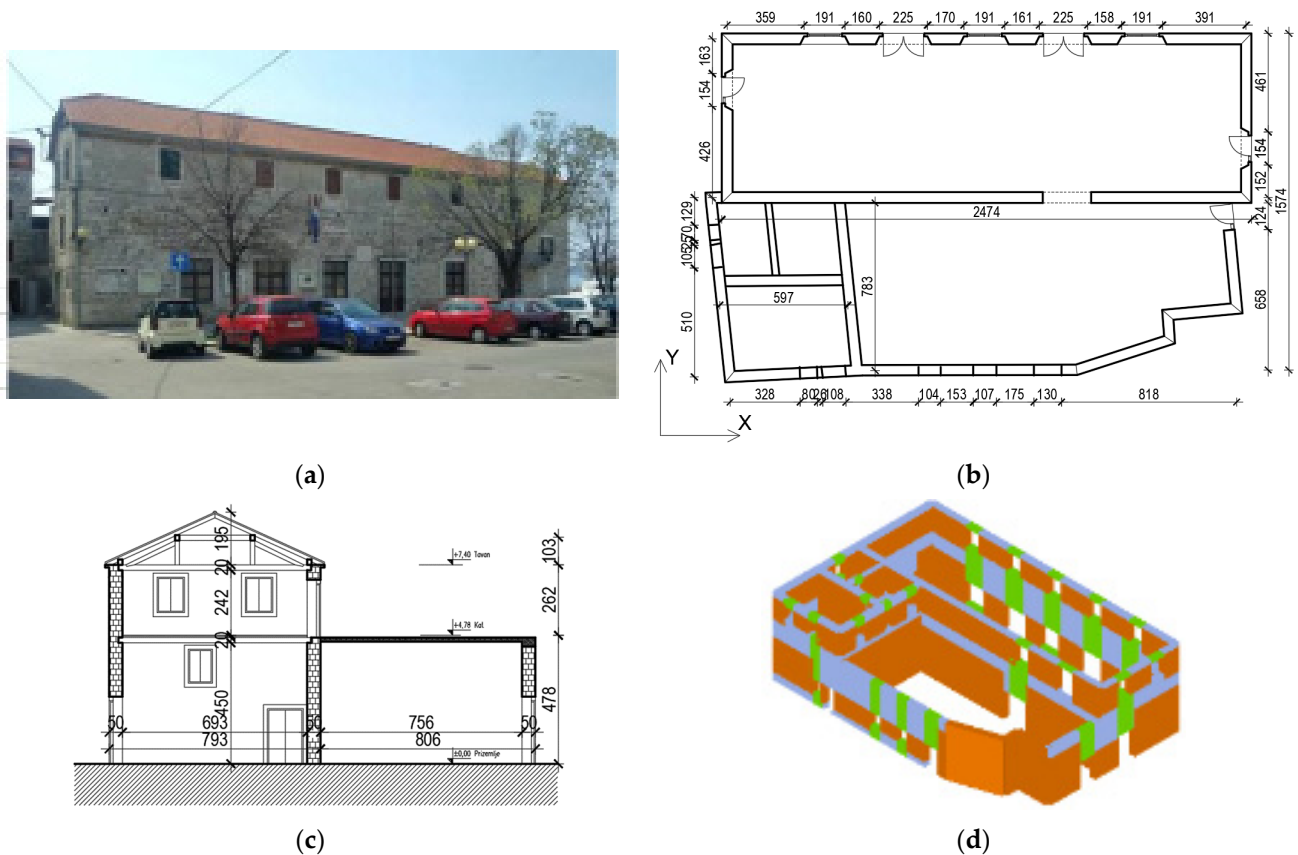


**Figure 12.** Public library: (a) photo of the building; (b) ground floor plan; (c) section view; (d) structural model used for non-linear seismic analysis.

The floors were modeled as flexible. The material properties of the walls were estimated according to [41], considering the results of in situ tests of the heritage building walls [42]. The mechanical material properties of the Public Library were assumed as an average of the reference values for building walls made of cut stone masonry with good bonding [41] as follows: compressive strength 2.60 MPa, tensile strength 0.10 MPa, modulus of elasticity 1700 MPa, shear modulus 580 MPa, and specific weights 21 kN/m<sup>3</sup>. A limited knowledge level (KL1) of the building and a confidence factor of CF = 1.35 according to EC8-3 [48] were assumed.

The seismic demand was defined by the elastic acceleration response spectrum. A type 1 response spectrum [46] and soil class A [46] were used for the test site. The input parameters taken in the seismic analysis were the importance factor  $\gamma_1 = 1.2$ , the design ground acceleration  $a_g = 0.22$  g, and the soil factor  $S = 1.0$ . Figure 13 shows the results of a total of 36 pushover analyses. The behavior was different along the two main directions and depended on the direction of the lateral loads.

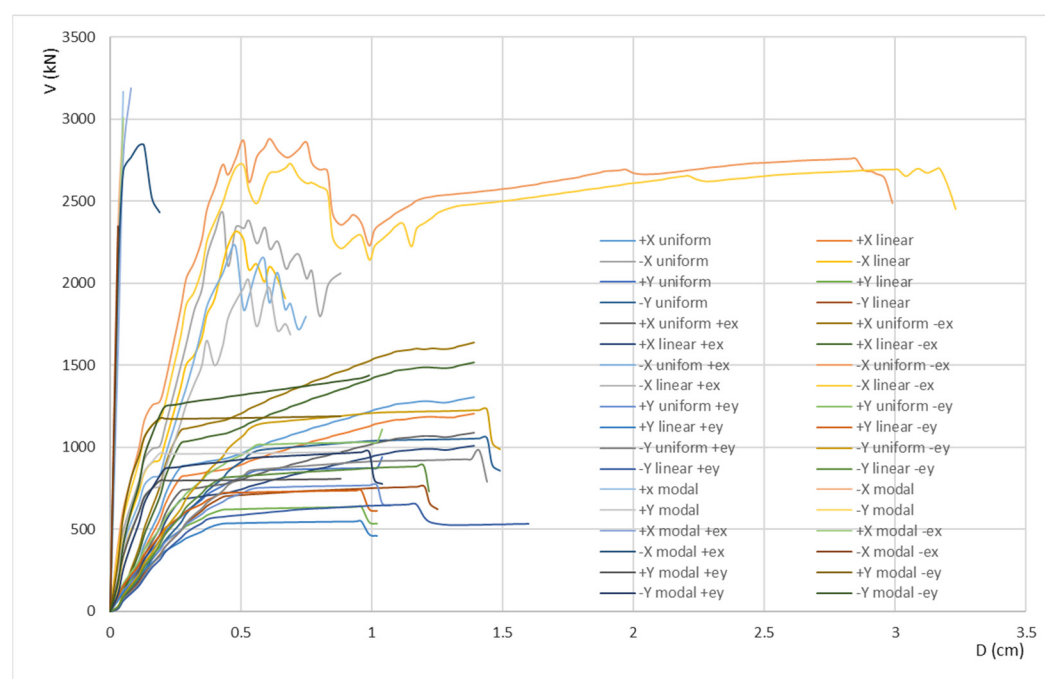


**Figure 13.** Pushover curves for the Public Library building.

The seismic capacity was evaluated, comparing the displacement capacity and the displacement demand obtained through a pushover analysis for the same control point. This procedure was performed for each of 36 cases and for two orthogonal directions (Table 2).

**Table 2.** Values of  $PGA_y$  and  $PGA_c$ .

Direction	Load	Eccentricity	$PGA_y/g$	$PGA_c/g$
+x	uniform	0	0.063	0.148
+x	linear	0	0.057	0.144
+x	modal	0	0.257	0.264
−x	uniform	0	0.121	0.188
−x	linear	0	0.121	0.147
−x	modal	0	0.235	0.257
+y	uniform	0	0.046	0.095
+y	linear	0	0.033	0.088
+y	modal	0	0.051	0.168
−y	uniform	0	0.054	0.132
−y	linear	0	0.039	0.105
−y	modal	0	0.060	0.173
+x	uniform	+5%	0.052	0.130
+x	uniform	−5%	0.079	0.171
+x	linear	+5%	0.048	0.123
+x	linear	−5%	0.072	0.166
+x	modal	+5%	0.248	0.264
+x	modal	−5%	0.231	0.245
−x	uniform	+5%	0.109	0.151
−x	uniform	−5%	0.143	0.553
−x	linear	+5%	0.098	0.131
−x	linear	−5%	0.136	0.557
−x	modal	+5%	0.229	0.413



−x	modal	−5%	0.207	0.208
+y	uniform	+5%	0.040	0.089
+y	uniform	−5%	0.055	0.107
+y	linear	+5%	0.028	0.079
+y	linear	−5%	0.038	0.100
+y	modal	+5%	0.042	0.144
+y	modal	−5%	0.066	0.212
−y	uniform	+5%	0.048	0.118
−y	uniform	−5%	0.063	0.146
−y	linear	+5%	0.031	0.122
−y	linear	−5%	0.045	0.115
−y	modal	+5%	0.049	0.156
−y	modal	−5%	0.071	0.194

The pushover curves which give the lowest capacity accelerations  $PGA_c$  in the x and y directions are shown in Figure 14, together with their bilinear idealizations, which are essential for capacity identification. The lowest capacity in both directions was obtained for the linear distribution.

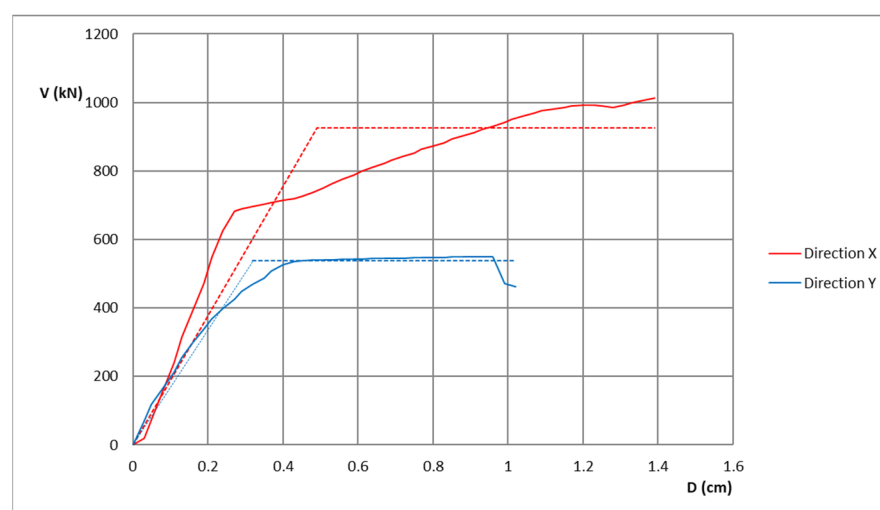


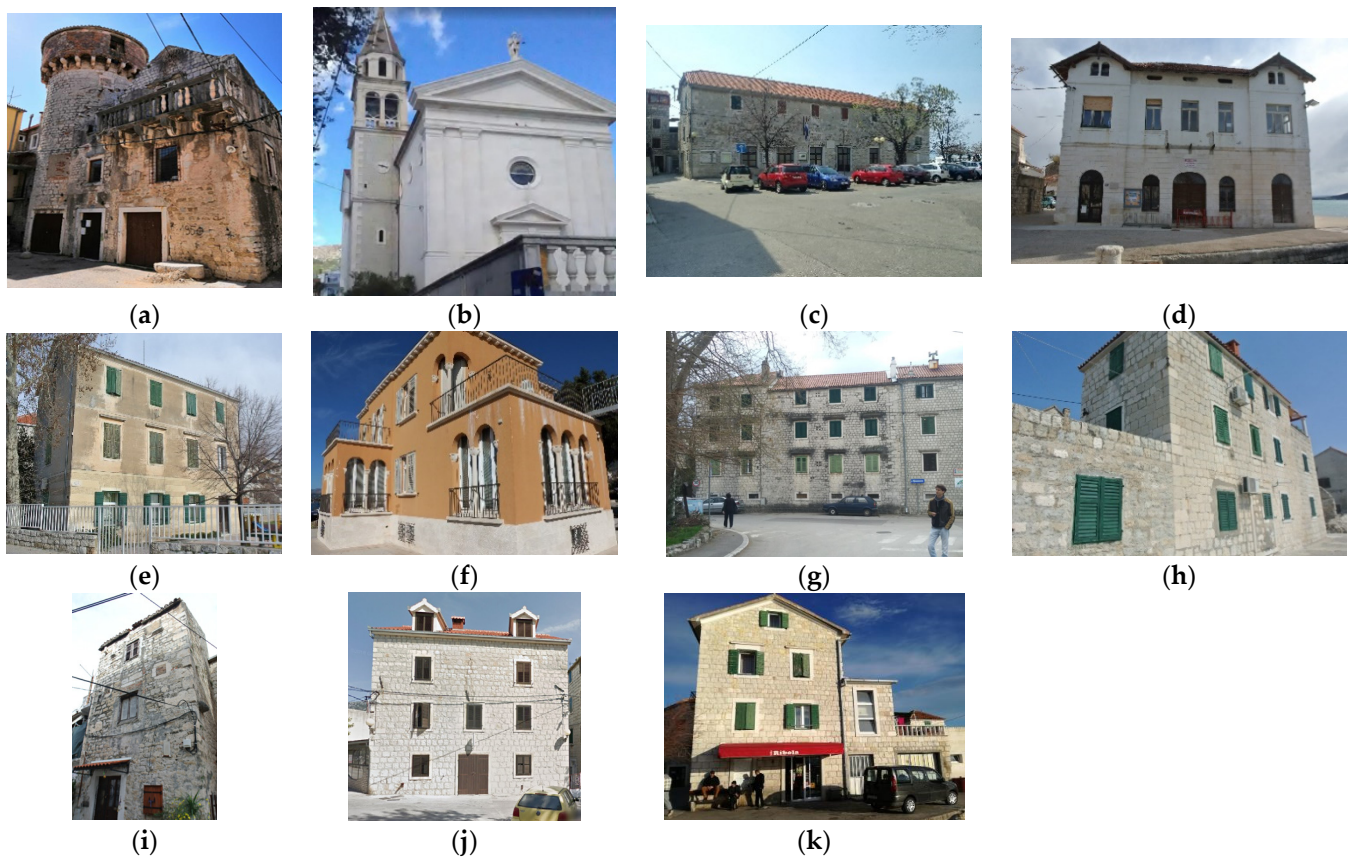
**Figure 14.** The worst cases of pushover curves.

The peak ground accelerations associated with the collapse limit state were computed according to EC8 [46]. The capacity acceleration in terms of the collapse for the case study is equal to 0.123 g (0.561  $a_g$ ) in the x direction and 0.079 g (0.363  $a_g$ ) in the y direction, where  $a_g$  represents the design ground acceleration, defined by the seismic hazard map for the return period of 475 years, and it is equal to  $a_g = 0.22$  g.

The same procedure was applied to obtain the peak ground accelerations  $PGA_y$ , corresponding to the yield point. It is worth mentioning that the lowest values of  $PGA_y$  and  $PGA_c$  do not necessarily correspond to the same distribution of lateral forces. In this case, the capacity acceleration in terms of the yield is equal to 0.048 g (0.218  $a_g$ ) in the x-direction and 0.028 g (0.130  $a_g$ ) in the y-direction.

Local mechanism failure was also analyzed to check local mechanisms such as those induced by a lack of connection among perpendicular walls, and poor connections among floors/roofs and walls. In the case of the Public Library building, the analysis showed that the lowest value of the failure acceleration for the local mechanism is 0.130 g. Hence, critical acceleration was obtained through global failure analysis.

With this procedure, 11 typical buildings (Figure 15) at the historical core were analyzed. The results of the pushover analysis and vulnerability indexes for the analyzed buildings are shown in Table 3.

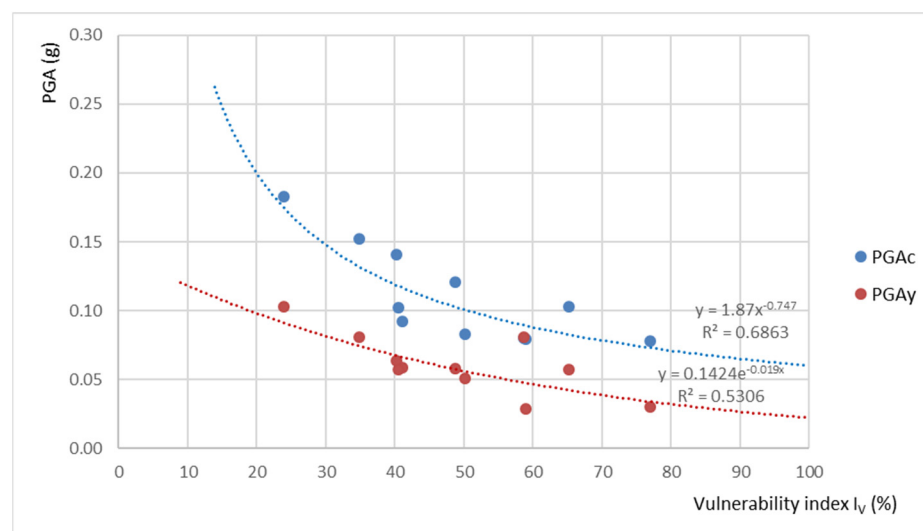


**Figure 15.** Analyzed buildings: (a) Cambi Tower; (b) St. Mihovil Church; (c) Public Library; (d) Rowing club; (e) Kindergarten; (f) Ballet School; (g) Dudan Palace; (h) Folk Castle; (i) Kumbat Towers; (j) Residential building—Obala kralja Tomislava 1; (k) Perišin house.

**Table 3.** Vulnerability index, yield acceleration, and collapse acceleration of the buildings.

Building	Vulnerability Index $I_v$ [%]	Yield Acceleration $PGA_y$ [g]	Collapse Acceleration $PGA_c$ [g]
Cambi Tower	76.9	0.030	0.078
St. Mihovil Church	40.5	0.057	0.102
Public Library	59.0	0.028	0.079
Rowing club	40.2	0.064	0.141
Kindergarten	41.0	0.059	0.092
Ballet School	23.9	0.103	0.183
Dudan Palace	50.1	0.051	0.083
Folk Castle	58.7	0.081	0.080
Kumbat Towers	65.2	0.057	0.103
Residential building	34.8	0.081	0.152
Perišin house	48.7	0.058	0.121

Figure 16 shows the relationship between the vulnerability index and collapse/yield accelerations for 11 buildings at the test site. The cloud of points represents the sample of buildings analyzed with the pushover analysis. The trend lines  $I_v$ – $PGA_y$  and  $I_v$ – $PGA_c$  for the yield and collapse states were obtained. The most representative functions were chosen. They can be used to approximately evaluate the yield and collapse peak ground accelerations for the historic center of Kaštel Kambelovac.

**Figure 16.** Trend lines  $I_v$ – $PGA_y$  and  $I_v$ – $PGA_c$ .

The vulnerability indexes for the buildings at the test site and the trend lines shown in Figure 16 were used to obtain the peak ground accelerations for early damage and collapse state. Figure 17 shows the collapse accelerations for the buildings in the test site.



**Figure 17.** Map of collapse accelerations.

The next step is the definition of the vulnerability curves for the historical center. Tri-linear vulnerability curves (Figure 3) were determined using yield and collapse peak ground accelerations,  $PGA_y$  and  $PGA_c$ , obtained through Equation (2) and using the relation shown in Figure 16. As  $PGA_y$  and  $PGA_c$  are functions of the vulnerability index  $I_v$ , the values of  $PGA_y$ , corresponding to damage  $d = 0$ , and  $PGA_c$ , corresponding to damage  $d = 1$ , can be computed for each value of  $I_v$ . These vulnerability curves are shown in Figure 18.

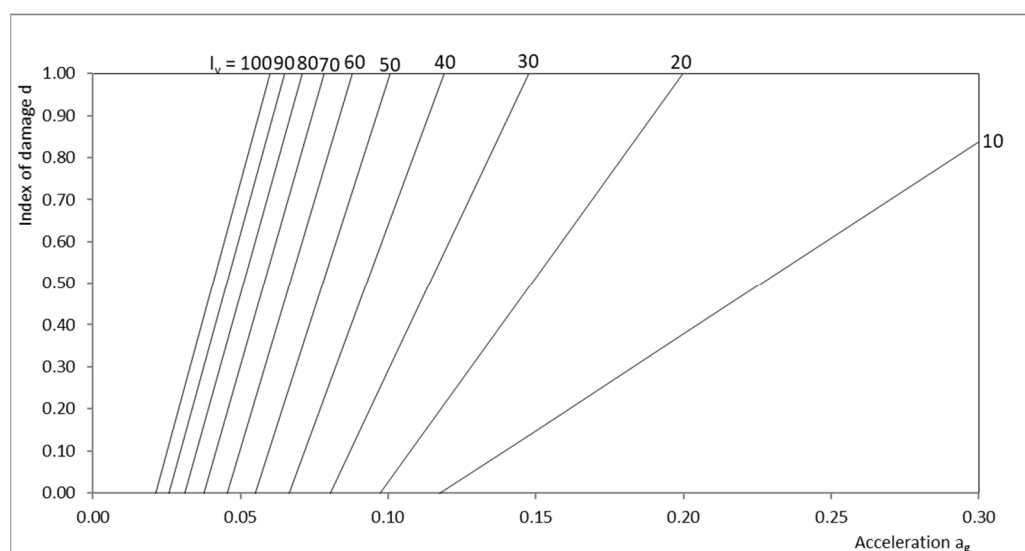


**Figure 18.** Vulnerability curves for the historic center of Kaštel Kambelovac.

The obtained vulnerability curves were exploited to define the damage index based on the vulnerability indexes. In the Kaštela area, the seismic hazard measured via the peak ground acceleration for the return periods of 475 and 95 years is equal to  $a_g = 0.22$  g and  $a_g = 0.11$  g for soil type A, respectively.

The damage indexes of the buildings were determined for the corresponding peak horizontal ground accelerations of 0.22 g and 0.11 g, and are presented in the maps in Figures 19 and 20.





Figure 19. Map of the damage index for  $PGA = 0.11$  g and a return period  $T = 95$  years.



Figure 20. Map of the damage index for  $PGA = 0.22$  g and a return period  $T = 475$  years.

#### 4. Discussion

A seismic vulnerability assessment approach based on the calculation of the seismic vulnerability indexes of the buildings was applied to the historical center of Kaštel Kamelovac, a Croatian city settlement placed along the coastal Dalmatian area. The approach consisted of the following stages:

- Identification of architectural, structural, and material characteristics of the buildings through the investigation of historical and archival documentation, literature, visual inspection, and thermographic imaging;
- Characterization of the soil type through a geophysical survey;
- Calculation of seismic vulnerability indexes for all buildings in the area;
- Calculation of the peak ground accelerations for early damage and collapse states of the buildings through non-linear static (pushover) analysis of representative buildings;
- Development of a new damage–vulnerability–peak ground acceleration relationship, which estimates the damage of the buildings under specific seismic action;
- Risk analysis in terms of seismic damage;

- Demonstration of seismic vulnerability and seismic risk using seismic vulnerability index maps and damage index maps.

Two main results were obtained from the investigation. The first one is the proposal of a methodology that allows the damage assessment of the building stock on a territorial scale for a certain seismic action expressed in terms of peak ground acceleration. This result was achieved by combining an expeditious empirical method based on vulnerability index calculation and detailed non-linear pushover analyses. The second result is the evaluation of vulnerability and risk in terms of the damage to stone masonry buildings in a typical historical city center located along the Croatian part of the Adriatic coast.

Furthermore, the relevant findings of this analysis are detailed as follows.

The obtained vulnerability indexes showed that most buildings (72.4%) belonged to medium-high ( $45 < I_v < 60$ ) and high ( $I_v > 60$ ) vulnerability classes. The reasons for such a high vulnerability are that these buildings cannot effectively bear the seismic load due to the fact that they were constructed with unconfined stone masonry walls, flexible wooden floors and roofs, and poor connections between the walls and floors. Additionally, irregularities in the plan and elevation, age, and the degree of general preservation of the building contribute to their high vulnerability. It has also been shown that reconstructed buildings have significantly lower vulnerability indexes. For example, one of the reconstructed buildings has a vulnerability index of 11.1.

The non-linear static (pushover) analysis carried out on 11 typical buildings indicated the low capacity of the buildings in terms of collapse peak ground acceleration (between 0.078 g and 0.183 g), as well as low accelerations of early damage states (between 0.029 g and 0.103 g). Generally, numerical predictions of the collapse acceleration by means of non-linear static analyses showed that no building meets the seismic requirement equal to  $a_g = 0.22$  g for  $T = 475$  years in either direction. Moreover, a significant number of buildings achieved collapse at accelerations that are lower than the demand acceleration of  $a_g = 0.11$  g for a return period  $T = 95$  years. These evaluations rely on the analysis of the global structural response. Evaluation of the local failure mechanisms for the Public Library building and a few other buildings showed that the lowest critical acceleration was obtained for the global response. Therefore, the yield and collapse acceleration and the associated damage for all buildings were estimated based on the global response of the structure. The motivation for this is that, considering that our final aim is a large-scale vulnerability assessment of the area, a global structural analysis is acceptable.

It is worth mentioning that the damage evaluation of the building was performed via static nonlinear analysis. Thus, the numerical damage patterns for the collapse acceleration do not necessarily comply with the damage to the structure caused by a real earthquake for the same acceleration. Numerical collapse is realized when the critical criteria for shear, compression, tension, and/or bending failure are achieved. The number of elements with realized failure criteria depends on the characteristics of the building, and can affect the damage intensity and damage pattern. Additionally, the results of the analysis depend on the material mechanical properties of the buildings, which are unknown. In fact, the mechanical properties were obtained from the literature and were reduced by a confidence factor equal to 1.35 according to Eurocode 8-3 [48]. The limitations of pushover analysis and the selection of control points could also influence the results in the case of horizontal and vertical irregularities. Despite these approximations and assumptions, the obtained results provide a better insight into individual seismic vulnerability, the capacity and expected damage of the buildings subjected to certain seismic actions, than the insights that can be reached by simply associating buildings to a class and then determining vulnerability and damage for the whole class. The results have important operational outcomes in terms of the planning and management activities for the investigated site. They can be used to determine priorities in rehabilitation and in the provision of funds for the reconstruction of the buildings.

Future efforts will be devoted to developing vulnerability and damage curves for the whole settlement, which includes not only the historical center with stone masonry buildings, but also newer buildings at the periphery, dating from the beginning of the 20th century to the present day.

## 5. Conclusions

This paper presents a procedure for assessing the seismic vulnerability of the historical center of Kaštel Kambelovac, one of the settlements of Kaštela City located along the Adriatic coast. The settlement has a typical configuration and buildings that are representative of other small and medium historical centers in Dalmatia, not only along the coast, but also inland. A detailed investigation of archival documentation and visual inspections were carried out to detect the main architectural, structural, and material features important for seismic vulnerability assessments. The proposed approach combines the calculation of the vulnerability index through numerical investigations of the behavior of typical buildings with non-linear pushover analysis. This procedure provides vulnerability index maps of the area, critical peak ground accelerations for the calculation of early damage and collapse states, and new vulnerability curves, which relate vulnerability index, peak ground accelerations, and the damage index. The derived vulnerability curves allow us to estimate the damage to buildings in the event of a specific seismic action. The damage indexes were reported here in the form of vulnerability maps of the investigated area for two return periods according to EC8, 475 and 95 years. Damage indexes are fundamental to preventing and managing seismic risk in the relevant area.

In the present study, we investigated for the first time the vulnerability of stone masonry buildings with flexible wooden ceilings, typical of the Dalmatian coast area. Furthermore, a methodology for the calculation of the damage index based on vulnerability indexes and seismic action in terms of peak ground acceleration was presented. Finally, the described methodology can be applied to and calibrated with other historic settlements.

**Author Contributions:** Conceptualization, Ž.N. and E.B.; data curation, L.R. and N.O.Š.; formal analysis, L.R. and N.O.Š.; funding acquisition, Ž.N. and E.B.; investigation, Ž.N., L.R., N.O.Š., and E.B.; methodology, Ž.N., L.R., N.O.Š., and E.B.; software, L.R.; supervision, Ž.N. and E.B.; validation, L.R. and N.O.Š.; visualization, L.R. and N.O.Š.; writing—original draft, Ž.N. and E.B. All authors have read and agreed to the published version of the manuscript.

**Funding:** This research was funded by: (1) the EUROPEAN UNION, Programme Interreg Italy-Croatia (Project “Preventing, managing and overcoming natural-hazards risks to mitigate economic and social impact”—PMO-GATE); (2) the CROATIAN GOVERNMENT and the EUROPEAN UNION through the European Regional Development Fund—the Competitiveness and Cohesion Operational Programme (Project KK.01.1.1.02.0027).

**Institutional Review Board Statement:** Not applicable.

**Informed Consent Statement:** Not applicable.

**Data Availability Statement:** Not applicable.

**Conflicts of Interest:** The authors declare no conflict of interest.

## References

1. Fajfar, P.; Gašperšič, P. The N2 method for the seismic damage analysis of RC buildings. *Earthq. Eng. Struct. Dyn.* **1996**, *25*, 11–46.
2. Fajfar, P.; Eeri, M. A nonlinear analysis method for performance based seismic design. *Earthq. Spectra* **2000**, *16*, 573–592.
3. Vamvatsikos, D.; Cornell, C.A. Incremental Dynamic Analysis. *Earthq. Eng. Struct. Dyn.* **2002**, *31*, 491–514.
4. Kreslin, M.; Fajfar, P. The extended N2 method considering higher mode effects in both plan and elevation. *Bull. Earthq. Eng.* **2012**, *10*, 695–715.
5. Rossetto, T.; Elnashai, A. Derivation of vulnerability functions for European-type RC structures based on observational data. *Eng. Struct.* **2003**, *25*, 1241–1263.

6. Maniyar, M.M.; Khare, R.; Dhakal, R.P. Probabilistic seismic performance evaluation of non-seismic RC frame buildings. *Struct. Eng. Mech.* **2009**, *33*, 725–745.
7. Ioannou, I.; Douglas, J.; Rossetto, T. Assessing the impact of ground-motion variability and uncertainty on empirical fragility curves. *Soil Dyn. Earthq. Eng.* **2015**, *69*, 83–92.
8. Ripepe, M.; Lacanna, G.; Deguy, P.; De Stefano, M.; Mariani, V.; Tanganelli, M. Large-Scale Seismic Vulnerability Assessment Method for Urban Centres. An Application to the City of Florence. *Key Eng. Mater.* **2014**, *628*, 49–54.
9. Salgado-Galvez, M.A.; Zuloaga, R.D.; Velasquez, C.A.; Carreno, M.L.; Cardona, O.D.; Barbat, A.H. Urban seismic risk index for Medellín, Colombia, based on probabilistic loss and casualties estimations. *Nat. Hazards* **2016**, *80*, 1995–2021.
10. Aguado, J.L.P.; Ferreira, L.P.; Lourenco, P.B. The Use of a Large-Scale Seismic Vulnerability Assessment Approach for Masonry Façade Walls as an Effective Tool for Evaluating, Managing and Mitigating Seismic Risk in Historical Centres. *Int. J. Archit. Herit.* **2018**, *12*, 1259–1275.
11. Salazar, L.G.F.; Ferreira, T.M. Seismic Vulnerability Assessment of Historic Constructions in the Downtown of Mexico City. *Sustainability* **2020**, *12*, 1276.
12. Capanna, I.; Cirella, R.; Aloisio, A.; Alaggio, R.; Di Fabio, F.; Fragiocomo, M. Operational Modal Analysis, Model Update and Fragility Curves Estimation, through Truncated Incremental Dynamic Analysis, of a Masonry Belfry. *Buildings* **2021**, *11*, 120.
13. Battaglia, L.; Ferreira, T.M.; Lourenço, P.B. Seismic fragility assessment of masonry building aggregates: A case study in the old city Centre of Seixal, Portugal. *Earthq. Eng. Struct. Dyn.* **2021**, *50*, 1358–1377.
14. Lagomarsino, S.; Cattari, S.; Ottonelli, D. The heuristic vulnerability model: Fragility curves for masonry buildings. *Bull. Earthq. Eng.* **2021**, *19*, 3129–3163.
15. Giordano, N.; De Luca, F.; Sextos, A. Analytical fragility curves for masonry school building portfolios in Nepal. *Bull. Earthq. Eng.* **2021**, *19*, 1121–1150.
16. Capanna, I.; Aloisio, A.; Di Fabio, F.; Fragiocomo, M. Sensitivity Assessment of the Seismic Response of a Masonry Palace via Non-Linear Static Analysis: A Case Study in L'Aquila (Italy). *Infrastructures* **2021**, *6*, 8.
17. Whitman, R.V.; Reed, J.W.; Hong, S.T. Earthquake Damage Probability Matrices. In Proceedings of the 5th World Conference on Earthquake Engineering, Rome, Italy, 25–29 June 1973; Volume II, pp. 2531–2540.
18. Benedetti, D.; Petrini, V. Vulnerability of masonry buildings: Proposal of a method of assessment (in Italian). *L'industria Costruzioni* **1984**, *149*, 66–74.
19. GNDT-SSN. *Scheda di Espozione e Vulnerabilità e di Rilevamento Danni di Primo e Secondo Livello (Murata e Cemento Armato)*; GNDT-SSN: Rome, Italy, 1994. Available online: [https://protezionecivile.regione.abruzzo.it/files/rischio%20sismico/verifiche-Sism/Manuale\\_e\\_scheda\\_GNDT\\_II\\_livello.pdf](https://protezionecivile.regione.abruzzo.it/files/rischio%20sismico/verifiche-Sism/Manuale_e_scheda_GNDT_II_livello.pdf) (accessed on 26 April 2021.).
20. Di Pascuale, G.; Orsini, G.; Romeo, R.W. New developments in seismic risk assessment in Italy. *Bull. Earthq. Eng.* **2005**, *3*, 101–128.
21. Lagomarsino, S.; Giovinazzi, S. Macroseismic and mechanical models for the vulnerability and damage assessment of current buildings. *Bull. Earthq. Eng.* **2006**, *4*, 415–443.
22. Grunthall, G. *European Macroseismic Scale 1998 (EMS-98)*; Cahiers du Centre Européen de Géodynamique et Séismologie: Luxembourg, 1998; Volume 15.
23. Guagenti, E.; Petrini, V. The case of old buildings: Towards a new law damage-intensity (in Italian). In Proceedings of the IV ANIDIS Convention, Milan, Italy, 1989; Volume I, pp. 145–153.
24. Bernardini, A. *The Vulnerability of Buildings-Evaluation on the National Scale of the Seismic Vulnerability of Ordinary Buildings*; CNR-GNDT: Rome, Italy, 2000.
25. Giovinazzi, S. The Vulnerability Assessment and the Damage Scenario in Seismic Risk Analysis. Ph.D. Thesis, Department of Civil Engineering, Technical University Carolo-Wilhelmina, Braunschweig, Germany; Department of Civil Engineering, Faculty of Engineering, University of the Florence, Florence, Italy, 2005.
26. FEMA. *HAZUS Technical Manual*; Federal Emergency Management Agency: Washington, DC, USA, 1999.
27. Kircher, C.A.; Whitman, R.V.; Holmes, W.T. HAZUS earthquake loss estimation methods. *Nat. Hazards* **2006**, *7*, 45–59.
28. Moroux, P.; Bertrand, E.; Bour, M.; Le Brun, B.; Depinois, S.; Masure, P.; the RISK-UE Team. The European RISK-UE project: An advanced approach to earthquake risk scenarios. In Proceedings of the 13th World Conference on Earthquake Engineering, Vancouver, BC, Canada, 1–6 August 2004.
29. Silva, V.; Crowley, H.; Varum, H.; Pinho, R.; Sousa, R. Evaluation of analytical methodologies used to derive vulnerability functions. *Earthq. Eng. Struct. Dyn.* **2014**, *43*, 181–204.
30. Angeletti, P.; Bellina, A.; Guagenti, E.; Moretti, A.; Petrini, V. Comparison between vulnerability assessment and damage index, some results. In Proceedings of the 9th World Conference on Earthquake Engineering, Tokyo, Japan, 2–9 August 1988.
31. Vicente, R.; Parodi, S.; Lagomarsino, S.; Varum, H.; Da Silva, M. Seismic vulnerability and risk assessment: Case study of the historic city centre of Coimbra, Portugal. *Bull. Earthq. Eng.* **2011**, *9*, 1067–1096.
32. Ahs, G.; Adam, C. Rapid seismic evaluation of historic brick-masonry buildings in Vienna (Austria) based on visual screening. *Bull. Earthq. Eng.* **2012**, *10*, 1833–1856.
33. Ferreira, T.M.; Mendes, N.; Silva, R. Multiscale Seismic Vulnerability Assessment and Retrofit of Existing Masonry Buildings. *Buildings* **2019**, *9*, 91.
34. Atalić, J.; Šavor Novak, M.; Uroš, M. Seismic risk for Croatia: Overview of research activities and present assessments with guidelines for the future. *Grđevinar* **2019**, *10*, 923–947.

35. Hadzima-Nyarko, M.; Pavić, G.; Lešić, M. Seismic vulnerability of old confined masonry buildings in Osijek, Croatia. *Earthq. Struct.* **2016**, *11*, 629–648.
36. Hadzima-Nyarko, M.; Mišetić, V.; Morić, D. Seismic vulnerability assessment of an old historical masonry building in Osijek, Croatia, using Damage Index. *J. Cult. Herit.* **2017**, *28*, 140–150.
37. Gordana Pavić, G.; Bulajić, B.; Hadzima-Nyarko, M. The Vulnerability of buildings from the Osijek database. *Front. Built Environ.* **2019**, *5*, 1–14.
38. Cavaleri, L.; Di Trapani, F.; Ferreto, M.F. A new hybrid procedure for the definition of seismic vulnerability in Mediterranean cross-border urban areas. *Nat. Hazards* **2017**, *86*, 517–541.
39. Available online: [https://marinas.com/view/marina/eyc39lv\\_Kastel\\_Kambelovac\\_Harbour\\_Kastel\\_Gomilica\\_Croatia](https://marinas.com/view/marina/eyc39lv_Kastel_Kambelovac_Harbour_Kastel_Gomilica_Croatia) (accessed on 21 November 2020.).
40. Marasović, K. Kaštel Kambelovac. *Kaštela J.* **2003**, *7*, 35–61. (In Croatian)
41. Uranjek, M.; Žarnić, R.; Bokan-Bosiljkov, V.; Bosiljkov, V. Seismic resistance of stone masonry building and effect of grouting. *Građevinar* **2014**, *66*, 715–726.
42. Bosiljkov, V.; Kržan, M. Results of Laboratory and In-Situ Tests on Masonry Properties and Tables with Mechanical Parameters to Be Adopted in Numerical Modelling, PERPETUATE (ECFP7 Project), Deliverable D15. 2012. Available online: [www.perpetuate.eu](http://www.perpetuate.eu) (accessed on 26 April 2021).
43. Ferrini, M.; Melozzi, A.; Pagliuzzi, A.; Scarparolo, S. *Rilevamento della vulnerabilità sismica degli edifici in muratura, Manuale per la compilazione della Scheda GNDT/CNR di II livello, Versione modificata dalla Regione Toscana. S.l.;* Direzione Generale delle Politiche Territoriale e Ambientali, Settore—Servizio Sismico Regionale: Regione Toscana, Italy, 2003.
44. Herak, M. Croatian map of seismic hazards. In Proceedings of the IVth Conference of Croatian Platform for Disaster Risk Reduction, Zagreb, Croatia, 13 December 2012; pp. 4–12.
45. HRN EN 1998-1:2011. *Design of Structures for Earthquake Resistance. Part 1: General Rules, Seismic Actions and Rules for Buildings*; Croatian Standards Institute: Zagreb, Croatia, 2011.
46. The European Union Per Regulation. *EN 1998-1 Eurocode 8: Design of Structures for Earthquake Resistance—Part 1: General Rules, Seismic Actions and Rules for Buildings*; European Committee for Standardization CEN: Brussels, Belgium, 2004.
47. Bohm, G.; Da Col, F.; Accaino, F.; Meneghini, F.; Schleifer, A.; Nikolić, Ž. Characterization of shallow sediments in an urban area (Kaštela, Croatia) by analysis of P, SV and Sh seismic velocities using a tomographic approach. In Proceedings of the Near Surface Geoscience Conference & Exhibition 2020, Belgrade, Serbia, 30 August–3 September 2020.
48. Croatian Standards Institute. *HRN EN 1998-3 Eurocode 8: Design of Structures for Earthquake Resistance—Part 3: Assessment and Retrofitting of Buildings*; Croatian Standards Institute: Zagreb, Croatia, 2011.
49. Lagomarsino, S.; Penna, A.; Galasco, A.; Cattari, S. TREMURI Program: An equivalent frame model for the nonlinear seismic analysis of masonry buildings. *Eng. Struct.* **2013**, *56*, 1787–1799.
50. *TREMURI Software*, Professional version; S.T.A. DATA: Torino, Germany, 2019.